SOCIEDADE BRASILEIRA DE FÍSICA

GENERAL AND APPLIED PHYSICS

Hollow Core Photonic Crystal Fiber (PCF)–Based Optical Sensor for Blood Component Detection in Terahertz Spectrum

Mahmoud M. A. Eid[1] · Md. Ahasan Habib[2] · Md. Shamim Anower[2] · Ahmed Nabih Zaki Rashed[3]

Abstract
Hollow core photonic crystal fiber is suggested and analyzed in this article for the identification of different blood components present in human blood. In order to visualize the fiber and investigate the performance of that sensor based on COMSOL simulation software, the suggested fiber is numerically analyze in terahertz frequency spectrum from 1.5 to 3 THz to obtain higher relative sensitivity (RS) and NA as well as lower absorption loss and confinement loss (CL) for better sensing applications. The reported hollow core fiber provides better interaction of light and the analytes, so that extremely high RS is achieved at a particular geometric condition. Furthermore, extremely low CL and effective material loss (EML) with high numerical aperture (NA) can be achieved from the suggested sensor which paves the way to apply the fiber in numerous biomedical applications.

Keywords Terahertz waveguide · Relative sensitivity (RS) · Numerical aperture (NA) · Confinement loss (CL)

1 Introduction

Photonic crystal fiber (PCF) has become an essential part of modern technology. In recent years, PCF has become important topic due to its numerous advantages (e.g., high tensile strength, low absorption loss, large bandwidth, flexibility) [1]. It was only used in communication sectors for faster data transmission with higher security. The advanced technology has proved that slight modified PCF can be employed in numerous promising applications in our daily life. Recently, the optoelectronics researchers have suggested different structured PCFs as chemical sensor [2–4], pressure sensor [5, 6], humidity sensor [7], and pH sensor [8]. As well as this type of optical waveguide can be used as remote toxic gas and chemical sensor where human entrance is very difficult or dangerous. Due to high melting point of glass or host material of the PCF, it can be used as temperature sensor where the temperature is beyond tolerable scale for human being. The modern biomedical and biological technology is now getting more and more dependent on PCF as it can be used as blood group detector, cancer cell detector in both invasive and non-invasive ways, blood sugar detector [9–11], etc. The conventional methods which are used for different pathological tests and imaging require huge time to complete the procedure and acquire results [12].

On the other hand, by using PCF, these tests can be performed within a few minutes with higher accuracy. Actually, the light guiding mechanism inside of a PCF is depending on the core dielectric constant through which the light travels. If the dielectric properties of two samples are different, then the guiding mechanism will be different, and from the analysis of received light signal, the samples can be distinguished. Naturally, the human blood cells consist of red blood cells (RBCs) and white blood cells (WBCs) [9]. By the volume,

✉ Ahmed Nabih Zaki Rashed
ahmed_733@yahoo.com

Mahmoud M. A. Eid
m.elfateh@tu.edu.sa

Md. Ahasan Habib
habib.eee.116.ah@gmail.com

Md. Shamim Anower
md.shamimanower@yahoo.com

1 Department of Electrical Engineering, College of Engineering, Taif University, Taif, Kingdom of Saudi Arabia

2 Department of Electrical and Electronic Engineering, Rajshahi University of Engineering & Technology, Kazla 6204, Rajshahi, Bangladesh

3 Electronics and Electrical Communications Engineering Department, Faculty of Electronic Engineering, Menoufia University, Menouf 32951, Egypt

about 54.3%, 45%, and 0.7% of blood are plasma, RBCs, and WBCs respectively [9]. Moreover, in plasma, almost 90% blood component is water and the rest are the combination of proteins, ions, dissolved gases, nutrients, and wastes. As the dielectric properties of the blood components are different, so by using light-analyte interaction inside PCF, different parts can be identified [13]. Very recently, terahertz frequency band is effectively employed to numerous sensing applications where PCF is used as the guiding channel of the terahertz light signal. By filling, some selected the air holes in core/cladding of PCF with unknown analytes, and by analyzing the light signal after interacting the light with the analytes, the unknown anatytes can be identified [3].

Hollow core PCF offers better sensitivity because it provides large space for interaction between light and the analytes than the other types. However, numerous structured porous core and hollow core PCF were suggested by the researchers for different sensing applications. For the identification of unknown liquid which offered very high RS of 89%, 88%, and 86% for benzene, ethanol, and water, respectively [2], a slotted core kagome lattice microstructure fiber was suggested by Islam et al. for same type of chemical identification which offered maximum RS of 85.7% for benzene at 1.6 THz [14]. However, the Kagome lattice fabrication is very challenging. Chopra et al. offered a diamond-shaped PCF-based sensor for cancer tissue, diabetes, and blood component detection present in the blood [15]. A solid core silica-based PCF was suggested by Singh and Kaur in 2017 for blood components detection where a narrow ring was introduced around the solid core for the introduction of blood into the sensor [16].

The authors claimed that their suggested sensor will eliminate the problem of leakage of light towards the cladding. The suggested sensor exhibits high RS of 55.09%, 54.05%, 53.72%, 56.05%, and 66.47% for hemoglobin, RBCs, WBCs, plasma, and water, respectively. Furthermore, the suggested solid core blood component sensor showed very low CL of 8.1343×10^{-9} dB/m, 1.8134×10^{-8} dB/m, 1.1928×10^{-8} dB/m, 4.8787×10^{-7} dB/m, and 4.075×10^{-7} dB/m for water, WBCs, hemoglobin, plasma, and RBCs, respectively. After that, Ahmed et al. suggested a new kind of porous core PCF-based sensor for blood component spectroscopic application [17]. The suggested sensor clarified very high RS of 80.93%, 80.56%, 80.13% 79.91%, and 79.39% with low CL of 1.23×10^{-11} dB/m, 8.63×10^{-12} dB/m, 4.93×10^{-12} dB/m, 2.93×10^{-12} dB/m, and 1.13×10^{-12} dB/m for RBCs, hemoglobin, WBCs, plasma, and water, respectively, at 1.5 THz. Unfortunately, the author did not consider NA and effective absorption loss of the suggested sensor. Though the numerical results are very attractive, but the geometry of the suggested sensor is too much difficult in both core and cladding and may not be fabricated at all. Furthermore, the air holes are very much closer to each other which will make the accurate fabrication of the fiber complicated.

In this paper, a circular type hollow core PCF-based sensor is suggested where single circular type air hole is clarified in the core and four quarter circular air hole ring type are placed in the cladding. The hollow core will pave the way to interact the light signal with the blood components, and the sensor may provide better result than that of porous core. By tuning the geometric parameters at various operating frequencies, the sensing parameters and other guiding characteristics of the suggested sensor are extracted. The numerical results inform that the reported hollow core fiber provides extremely high RS of 95.80%, 95%, 93.60%, 92.50%, and 91.40% that are obtained for RBCs, hemoglobin, WBCs, plasma, and water, respectively at a particular geometric condition. Moreover, the suggested sensor offers very low CL and CL with high NA. By using modern fabrication techniques, the suggested fiber can be fabricated with higher accuracy.

2 Sensor Design Schematic View

The suggested fiber sensor schematic view is illustrated in Fig. 1; one circular type air hole is introduced with diameter $\mathbf{D_c}$ which will act as core in the central region. The analyte which is required to test will fill into that hole, and from the light-analyte interaction, the sensitivity will be calculated. Around the core, four quarter ring type air holes are introduced whose outer and inner radius are $\mathbf{r_{co}}$ and $\mathbf{r_{ci}}$, respectively. For simplicity, above two parameters are directly related to $\mathbf{D_C}$ where $\mathbf{r_{co}} = 2.75\mathbf{D_C}$ and $\mathbf{r_{ci}} = 0.55\mathbf{D_C}$. The strut thickness between two air holes cladding are denoted by $\mathbf{d}$, and it is 0.12 times of $\mathbf{D_C}$. All these values are selected by using trial-and-error method, and at this geometric condition, the suggested fiber offers excellent characteristics.

The analytes which are required to be tested will be filled in the core, and the values of dielectric constants of the blood components are taken from previous studies [9, 16, 17]. A circular perfectly matched layer (PML) boundary
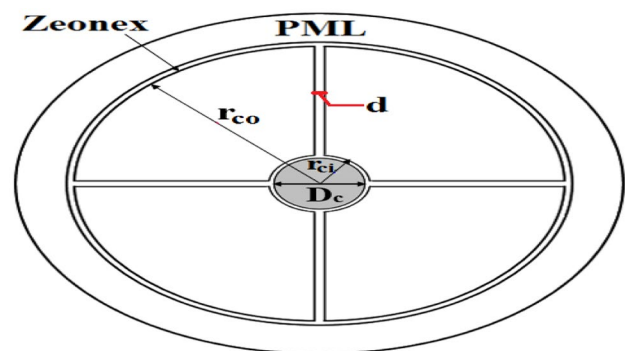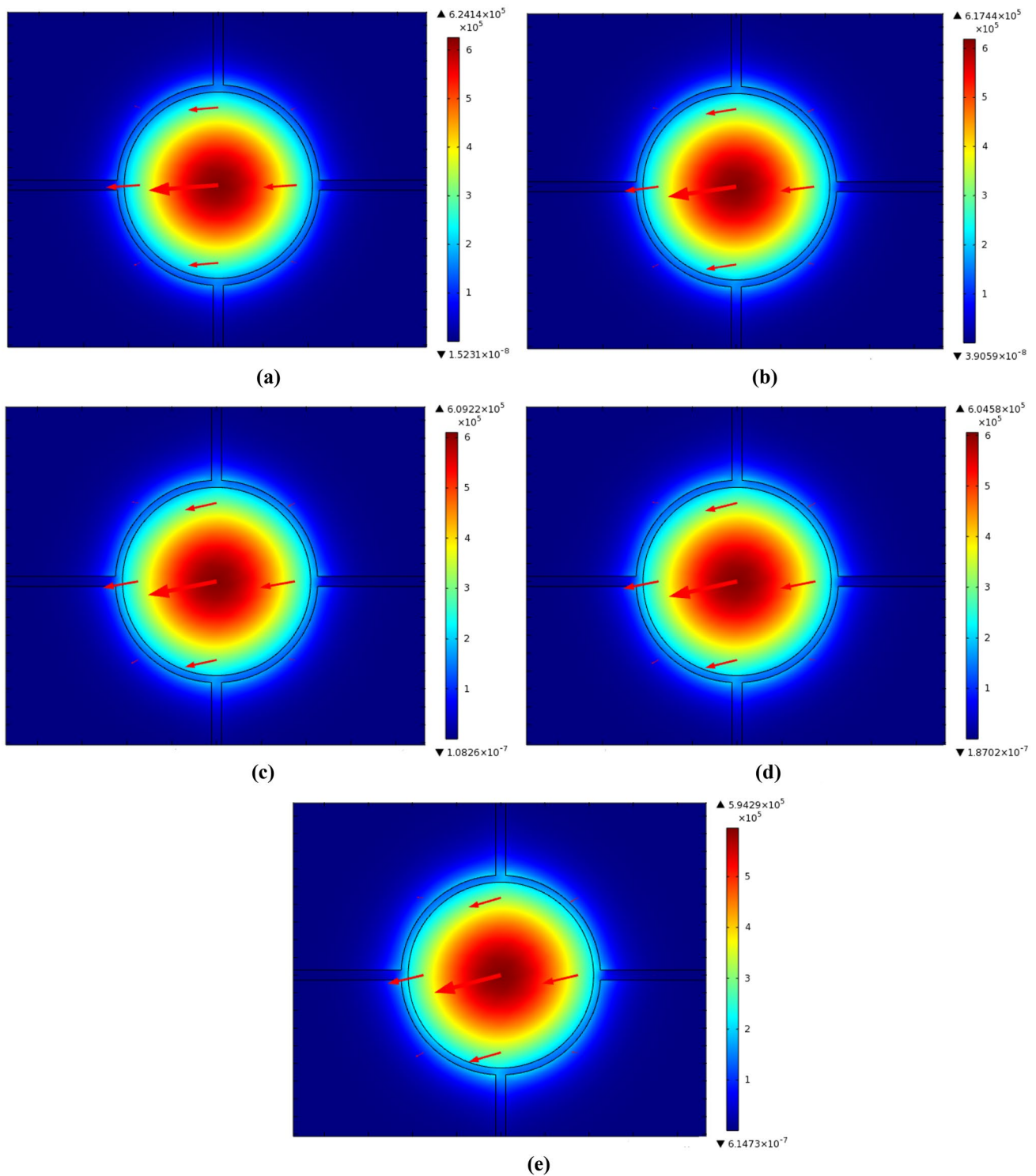

Fig. 1 The suggested hollow core fiber cross-sectional view

Fig. 2 Mode field distribution of the proposed sensor for **a** RBC, **b** Hemoglobin, **c** WBC, **d** plasma, and **e** water at 210 μm core diameter when $f = 2.7$ THz

condition is employed outside of the cladding region for absorbing the electromagnetic waves diverted from core to eliminate back reflection. In this suggested sensor, Zeonex is used as the background material for its excellent characteristics in terahertz regime. It offers lowest absorption loss (0.2 cm^{-1}) from 0.1 to 2 THz [2].

3 Simulation Results and Discussions

The mode field distribution of the proposed sensor with intensity scale is represented in Fig. 2 for all blood components. The intensity scale for all samples indicates that for RBC, the intensity of light through the core is maximum whereas minimum for water sample. This type of characteristics is shown by the sensor in accordance to the refractive index of the analyte.

To visualize the suggested fiber and investigate the characteristics as a sensor, COMSOL simulation software is employed. The key guiding parameters of any sensor such as RS, effective absorption loss, CL, and NA will be investigated in detail. It previously stated that the light guiding characteristics inside of a PCF is dependent on the dielectric constant of that core. If the RI varies, the amount of light propagation through the core will vary also. How much variation occurs due to the variation of RI is termed as RS. A sensor may be treated as good sensor if the RS is high. The mathematical expression to calculate the RS of a sensor is [17] eq. 1

$$r = \frac{n_r}{n_{\text{eff}}} \times P\% \tag{1}$$

where r is the RS; n_r and n_{eff} are the effective guided mode RI and the analytes, respectively; and the term P indicates power fraction. The power fraction is calculated by [17] Eq. 2

$$P = \frac{\int\limits_{\text{sample}} R_e(E_x H_y - E_y H_x)dxdy}{\int\limits_{\text{total}} R_e(E_x H_y - E_y H_x)dxdy} \times 100 \tag{2}$$

where E_x, E_y, H_x, and H_y are the electric field and magnetic fields, respectively, in x and y directions and the light propagates in z direction. The RS of the suggested fiber for different CD at 2.5 THz, 2.6 THz, and 2.7 THz are shown in Fig. 3. It is demonstrated for all operating frequencies and

blood components that the RS increases with the increase of CD till $D_C = 210$ μm, and after that, the RS remain constant. This occurs because the increased CD offers more light-analyte interaction and that is why the RS increases. When the CD is 210 μm, then maximum light-analyte interaction occurs and further increased CD provide more space for electromagnetic signal but the light-analyte interaction remains constant.

At a fixed frequency and CD, the RS is highest for RBCs and lowest for water due to the effective RI of the analyte. As the RI of RBCs is highest among the analytes and that is why maximum light propagates through the core for RBCs which increases the sensitivity. Again, the RS for a fixed geometric condition increases based on the operating frequency increase which is clarified in Fig. 4. This figure indicates that the RS is maximum at 2.7 THz for all blood components so that 2.7 THz is taken as optimum operating frequency. For that suggested sensor, $D_C = 210$ μm is the optimum CD because at that condition the RS is maximum and the sensitivity is almost constant when the CD is larger than that. The RS of the suggested sensor are 95.80%, 95%, 93.60%, 92.50%, and 91.40% for RBCs, hemoglobin, WBCs, plasma, and water, respectively at $D_c = 210$ μm and operating light frequency is 2.7 THz.

Though RS is the key parameter of a sensor, there is another important parameter of any kind of optical fiber based sensor. This parameter indicates the amount the power loss due the absorption of light by the cladding air holes surrounding the core. Lower CL is desirable and this parameter is cast by [16], eq. 3

$$\alpha_{\text{CL}} = 8.686 \times \frac{2\pi f}{c} \text{Im}(n_{\text{eff}}) \tag{3}$$

where $\text{Im}(n_{\text{eff}})$ is imaginary part of the guided mode RI. The sketch of the CL for the suggested fiber at various geometric configuration is illustrated in Fig. 5 for $f = 2.5$ THz (solid line), $f = 2.6$ THz (dashed line), and $f = 2.7$ THz (dotted line).

Fig. 3 RS of the suggested hollow core sensor as a function of CD
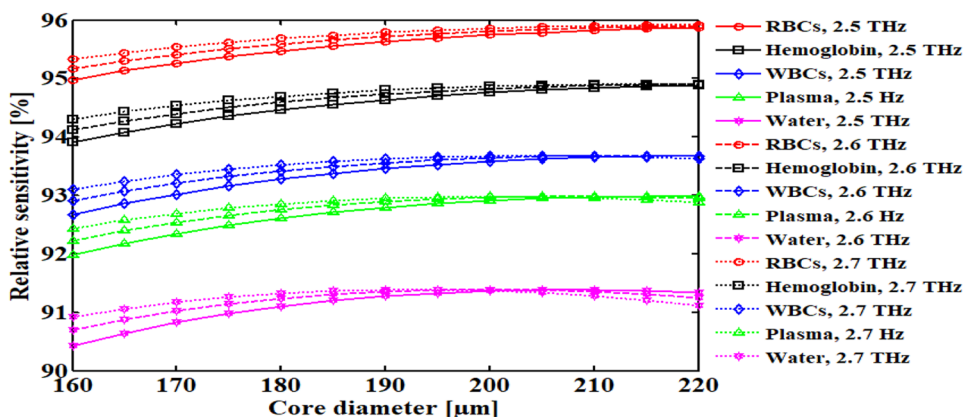
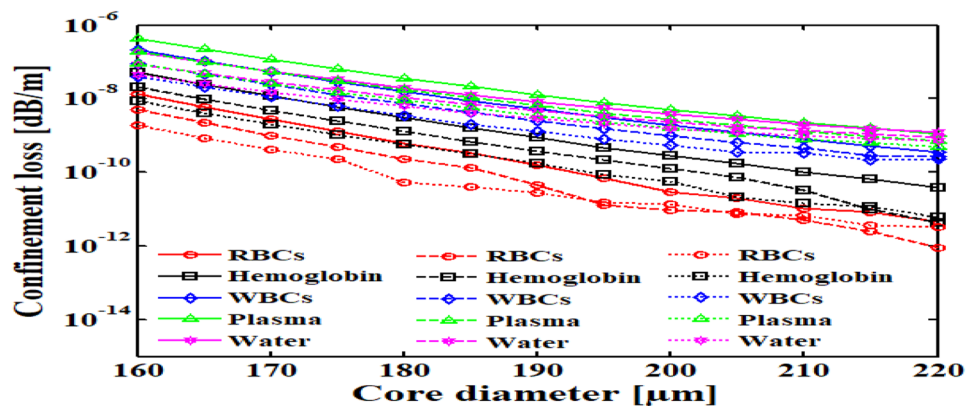**Fig. 4** RS of the suggested fiber for various operating frequencies at $D_C = 210$ μm
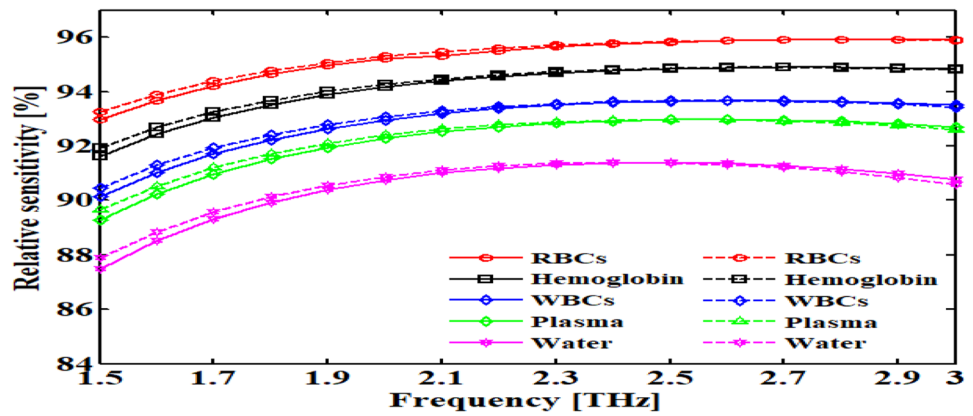
From the following figure, it is clear that at any particular CD, the CL is lower at higher operating frequencies. Moreover, the CL characteristics is also represented as a function of operating frequencies is illustrated in Fig. 6 also. As previously mentioned, the higher frequency EMW always tries to travel through the higher RI zone so at high frequency more light signal travels through the core. The fraction of light at cladding reduces at higher frequency which is responsible for reducing the CL. At 2.7 THz, the CL of the suggested fiber for different blood components are 3.80×10^{-11} dB/m, 1.13×10^{-11} dB/m, 2.15×10^{-10} dB/m, 6.25×10^{-10} dB/m, and 8.30×10^{-9} dB/m, respectively, for RBCs, hemoglobin, WBCs, plasma, and water which are lower than the previously clarified works [9, 16, 17].

The length of the suggested fiber is not too long but the EML characteristics will be investigated in order to clarify about the required minimum incident light energy from the light source. The equation which is used to evaluate the EML of any optical waveguide is [2] eq. 4

$$\alpha_{\text{eff}} = \frac{\left(\varepsilon_0/\mu_0\right)^{1/2} \int_{A_{\text{mat}}} n\alpha_{\text{mat}} |E|^2 dA}{2 \int_{\text{All}} S_z dA} \qquad (4)$$

where ε_0 indicates the relative permittivity of free space, μ_0 is for the relative permeability of vacuum, n is the RI of the guided light, E is the modal electric field, S_z is for the Poynting vector in z direction, and α_{mat} is the material loss coefficient of the background material which is 0.2 cm^{-1} for Zeonex. The numerator performs the calculation of power absorbed by the material only where the denominator provides the information about total power present inside of the waveguide. This loss characteristics of the suggested blood component sensor is illustrated in Fig. 7, based on the frequency for 210 μm and 215 μm CD. This figure indicates that the material loss decreases based on the light signal frequency increase and almost constant after 2.5 THz except for water substance. At higher frequency more light travels through high RIed blood components rather than the air and the loss reduces. The EML for that suggested sensor is 0.015 cm^{-1}, 0.013 cm^{-1}, 0.012 cm^{-1}, 0.01 cm^{-1}, and 0.009 cm^{-1} at 2.7 THz for RBCs, hemoglobin, WBCs, plasma, and water, respectively. If the EML is high and weak signal provided by the source, then the detector at the opposite side of the source may not receive any light due to the attenuation of light by the material. That is why lower EML is desirable so that low powered light source can be implemented with the sensor.

Fig. 5 CL as a function of CD at 2.5 THz (solid line), 2.6 THz (dashed line), and 2.7 THz (dotted line)

Fig. 6 CL of the suggested fiber for various operating frequencies when $D_C = 210$ μm (solid line) and $D_C = 215$ μm (dashed line)
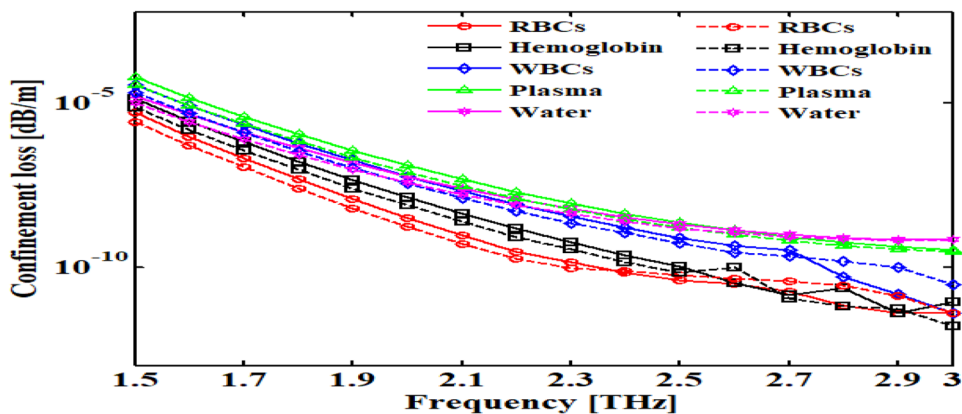
NA is a vital parameter for PCF-based optical waveguides. This parameter informs about the range of the angle of incident light signal which can travel through the waveguide. For broad sensing applications, the value of NA should be as high as possible. The mathematical expression to calculate NA is given below [2], eq. 5

$$NA = \frac{1}{\sqrt{1 + \frac{\pi A_{eff} f^2}{c^2}}} \qquad (5)$$

where A_{eff} is the guided light signal effective area. This parameter illustrates the amount of area where the light propagates. This parameter can be quantified by [2] eq. 6

$$A_{eff} = \frac{\left[\int I(r) r dr\right]^2}{\left[\int I^2(r) dr\right]^2} \qquad (6)$$

where $I(r)$ represents the electric field density of the fiber cross sectional transverse and r is the core radius. Figure 8 illustrates the relationship of effective area of the suggested sensor for different core dimension as a function of frequency. As higher frequency, light travels more through the higher RIed core so the effective area decreases based on the increase of operating frequency. The lower effective area indicates tight light confinement within the core which means better light-analyte interaction inside the core. In case of sensing applications, lower effective area is desirable as if maximum light energy travels through small area, then the light-analyte interaction will be maximum as well as the EML and confinement loss will be lower also. If the effective area increases, then more light propagate through the cladding air holes and the loss will be increased. As a result, the RS is higher at high operating frequencies. The NA variation of the suggested sensor for various operating frequencies is illustrated in Fig. 9. This sketch illustrates that at a fixed operating frequency, the NA is higher for higher CD as the enlarged CD accepts more light to travel through it. Moreover, the acceptance angle of the suggested PCF decreases based on the frequency increase for any geometric dimension. The NA of the suggested optical sensor fiber is almost 0.38 at 2.7 THz when the CD is 210 μm which is satisfactory for any kind of sensor.

Another essential parameter of a sensor is the modal spot size which is closely related to the normalized frequency parameter. For better sensing application, larger spot size is desirable. The spot size is cast by [17] eq. 7

$$W_{eff} = R \times (0.65 + 1.619 \times V^{-1.5} + 2.879 \times V^{-6}) \qquad (7)$$

Fig. 7 CL of that suggested sensor for various operating frequencies at $D_C = 210$ μm (solid line) and $D_C = 215$ μm (dashed line)
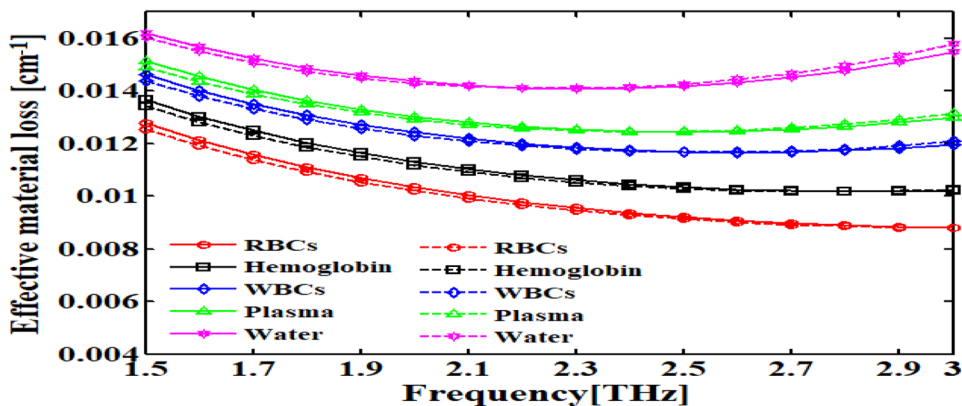
Fig. 8 Effective area of that suggested sensor at various operating frequencies for $D_C = 210$ μm (solid line) and $D_C = 215$ μm (dashed line)
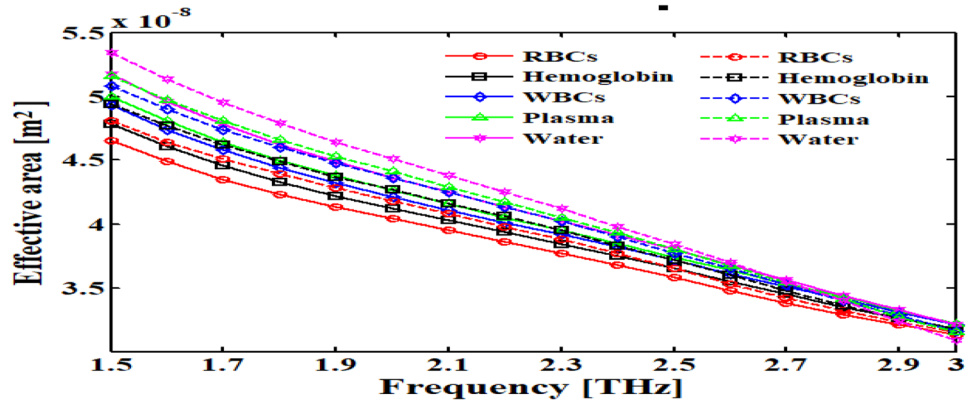
where, R is the core air hole radius and V is the normalized value of V_{eff} parameter. The numerical value of V is given by [17], eq. 8

$$V_{eff} = \frac{2\pi r f}{c} \sqrt{n_{co}^2 - n_{cl}^2} \qquad (8)$$

where n_{co} and n_{cl} are for the core-cladding section effective RI of respectively and the value of V_{eff} must be less or equal to 2.405 for single-mode operation. The value of n_{co} can be directly calculated based on simulation program, but the value of n_{cl} can be directly calculated from the software. As high air filling fraction is used in the suggested design, so the value of n_{cl} is 1.06. The graphical representation of normalized V parameter is illustrated in Fig. 10 at different operating frequency. After that, Fig. 11 illustrates the spot size of the suggested sensor for various operating frequencies at 210 μm and 215 μm CD. The figure illustrates that the spot size decreases with the operating frequency increase at

a fixed CD because the effective area is lower at higher operating frequencies. The spot size is almost 86 um for all blood components at 2.7 THz of the suggested optical waveguide.

Finally, the suggested fiber fabrication technique is presented. In the cladding region, four quarter-circular-shaped air holes are introduced where a circular air hole is inserted at the central portion of the suggested fiber. In recent years, numerous porous core and hollow core PCF have been fabricated by using various fabrication techniques including drilling, stack and draw, capillary stacking, and sol–gel technique [2, 16, 17]. We hope anyone method from the previously mentioned techniques can be used to produce the suggested sensor. Now, it is high to compare our suggested sensor with recently published article in Singh and Kaur [16] and Ahmed et al. [17] which will be shown in Table 1. From the chart, it is clear that our suggested sensor is better than Singh and Kaur [16] and Ahmed et al. [17].
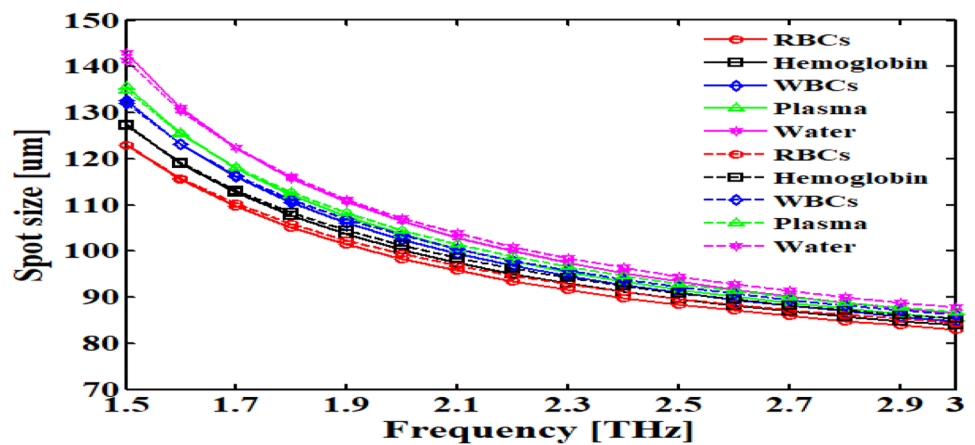
Fig. 9 NA of that suggested microstructure fiber at different operating frequencies for $D_C = 210$ μm (solid line) and $D_C = 215$ μm (dashed line)
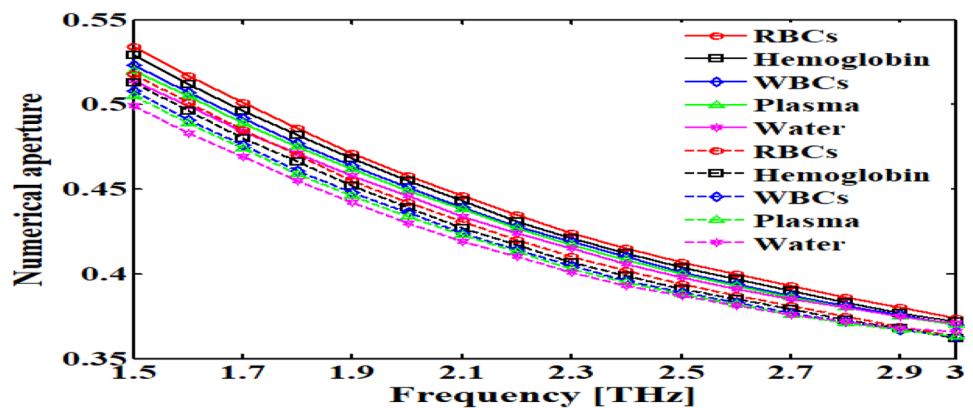
Fig. 10 V parameter of the suggested fiber-based operating frequencies at $D_C = 210\ \mu m$ (solid line) and $D_C = 215\ \mu m$ (dashed line)
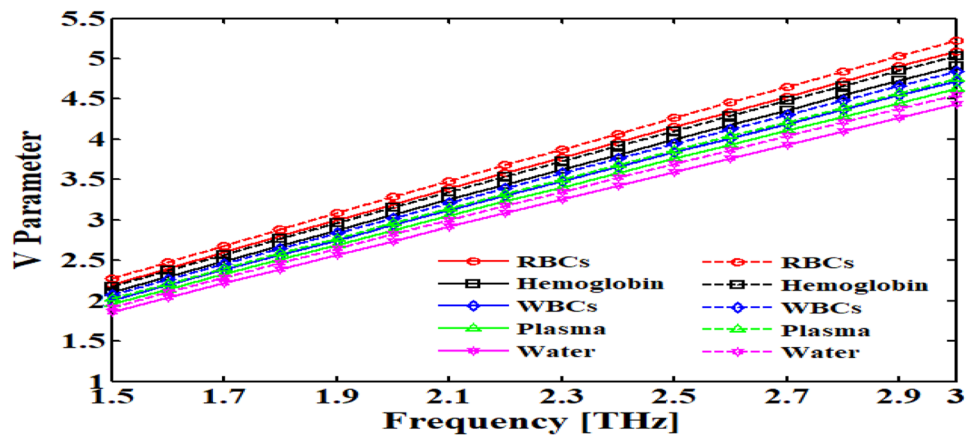
Fig. 11 Spot size of the suggested fiber-based operating frequencies at $D_C = 210\ \mu m$ (solid line) and $D_C = 215\ \mu m$ (dashed line)

Table 1 Guiding properties of the suggested sensor with recently published optical fiber based sensor

Ref	Year	Background material	Component name	Relative sensitivity (%)	Confinement loss (dB/m)	NA	Spot size (μm)
[16]	2017	Silica	RBCs	56.05	4.075×10^{-7}	–	–
			Hemoglobin	66.47	1.1928×10^{-8}	–	–
			WBCs	53.72	1.8134×10^{-8}	–	–
			Plasma	54.05	4.8787×10^{-7}	–	–
			Water	55.09	8.1343×10^{-9}	–	–
[17]	2018	TOPAS	RBCs	80.93	1.23×10^{-11}	–	743
			Hemoglobin	80.56	8.63×10^{-12}	–	527
			WBCs	80.13	4.93×10^{-12}	–	375
			Plasma	79.91	2.93×10^{-12}	–	250
			Water	79.39	1.13×10^{-12}	–	200
This work	–	Zeonex	RBCs	95.8	3.80×10^{-11}	0.38	86
			Hemoglobin	95	1.13×10^{-11}	0.38	86
			WBCs	93.6	2.15×10^{-10}	0.38	87
			Plasma	92.5	6.25×10^{-10}	0.38	87
			Water	91.4	8.30×10^{-9}	0.38	87

4 Conclusion

This study clarified a hollow core PCF sensor investigated numerically for sensing different components present in the human blood. The numerical analysis reports that the suggested sensor offers very high RS of 95.80%, 95%, 93.60%, 92.50%, and 91.40% with low CL of 3.80×10^{-11} dB/m, 1.13×10^{-11} dB/m, 2.15×10^{-10} dB/m, 6.25×10^{-10} dB/m, and 8.30×10^{-9} dB/m, respectively, for RBCs, hemoglobin, WBCs, plasma, and water at optimum condition simultaneously. Along with this excellent guiding characteristics, the suggested sensor offers very low EML lower than 0.015 cm^{-1} and very high NA of 0.38 for all blood components at a same geometric parameter. The suggested sensor is very simple to realize with the fabrication easily through the recent technology. Therefore, this fiber may improve an essential part of biological sensing sectors.

5 Availability of Data and Material

The proposed sensor is numerically investigated by COMSOL simulation software.

References

1. M.A. Habib, M.S. Reza, L.F. Abdulrazak, M.S. Anower, Opt. Commun. **446**, 93–99 (2019)
2. M.A. Habib, M.S. Anower, L.F. Abdulrazak, M.S. Reza, Opt. Fib. Technol. **52**, 101933 (2019)
3. M.F.H. Arif, M.J.H. Biddut, Sens. Bio. App. **12**, 8–14 (2017)
4. B.K. Paul, S. Islam, K. Ahmed, S. Asaduzzaman, Photn. Sens. **7**, 123–130 (2017)
5. X. Wang, Q. Wang, Z. Song, K. Qi, AIP Advan. **9**(9), 095005 (2019)
6. W.J. Bock, J. Chen, P. Mikulic, T. Eftimov, M.K. Pawlowski, Meas. Sci. Technol. **18**(10), 3098 (2019)
7. J. Mathew, Y. Semenova, G. Rajan, G. Farrell, Electron. Lett. **46**(19), 1341–1343 (2010)
8. C. Wu, B. Guan, C. Lu, H. Tam, Opt. Express **19**(21), 20001–20008 (2011)
9. P. Sharma, P. Sharan, Opt. Commun. **348**, 19–23 (2015)
10. K. Kawase, Y. Ogawa, Y. Watanabe, H. Inoue, Opt. Express **11**(20), 2549–2554 (2003)
11. D. Abbott, X.C. Zhang, Proc. IEEE. **95**(8), 1509–1513 (2007)
12. T. Paillard, F. Noe, BioMed Res. Int. **891390**, 1–15 (2015)
13. M.S. Islam, J. Sultana, A. Dinovitser, K. Ahmed, B.W.H. Ng, D. Abbott, Opt. Commun. **426**, 341–347 (2018)
14. M.S. Islam, J. Sultana, K. Ahmed, M.R. Islam, A. Dinovitser, B.W.H. Ng, D. Abbott, IEEE Sens. J. **18**(2), 575–582 (2018)
15. H. Chopra, R.S. Kaler, B. Painam, J. Nanophotonics **10**, 036011 (2016)
16. S. Singh, V. Kaur, IEEE Int Conf. in Ubiquitous and Fut. Net. 399–403 (2017)
17. K. Ahmed, F. Ahmed, S. Roy, B.K. Paul, M.N. Akter, D. Vigneswaran, M.S. Islam, IEEE Sens. J. **19**, 3368–3375 (2019)